



## **A review of the effect of neutron irradiation on the deformation behaviour of copper and copper alloys**

**Forskningscenter Risø, Roskilde**

*Publication date:*  
1976

*Document Version*  
Publisher's PDF, also known as Version of record

[Link back to DTU Orbit](#)

*Citation (APA):*  
Higgy, H. R. (1976). A review of the effect of neutron irradiation on the deformation behaviour of copper and copper alloys. (Risø-M; No. 1871).

## **DTU Library** Technical Information Center of Denmark

---

### **General rights**

Copyright and moral rights for the publications made accessible in the public portal are retained by the authors and/or other copyright owners and it is a condition of accessing publications that users recognise and abide by the legal requirements associated with these rights.

- Users may download and print one copy of any publication from the public portal for the purpose of private study or research.
- You may not further distribute the material or use it for any profit-making activity or commercial gain
- You may freely distribute the URL identifying the publication in the public portal

If you believe that this document breaches copyright please contact us providing details, and we will remove access to the work immediately and investigate your claim.

CONTENTS

	Page
1. Introduction .....	5
2. Mechanism of Irradiation Hardening .....	5
3. Dose Dependence of CSS .....	7
4. Effect of Alloying on Irradiation Hardening .....	8
Copper-gold Alloys .....	8
Copper-Aluminium Alloys .....	10
5. Effect of Cold-work on Irradiation Hardening .....	11
6. Deformation on Neutron-Irradiated Copper and Copper Alloys .....	14
Pure Copper ::::::::::: .....	14
Copper Alloys .....	17
7. Conclusion .....	20
Acknowledgements .....	22
References .....	23
Figures .....	25

## 1. INTRODUCTION

It is well known that bombardment of metals by energetic neutrons induces considerable changes in their physical and mechanical properties. The increase in critical shear stress by irradiation (irradiation hardening) is due to the interaction of the irradiation-produced defects with dislocations. Several irradiation hardening studies have been performed on fcc metals especially copper<sup>(1-3)</sup>. At first, pure and well annealed metals were used. Later, the effects of alloying and pre-straining on irradiation hardening of copper were studied<sup>(4-5)</sup>.

The present report reviews the effect of neutron irradiation on the mechanical properties and the deformation behaviour of pure copper and copper alloys. The mechanism of irradiation hardening is described in section 2. In section 3, the neutron dose dependence of the critical shear stress is investigated. The contradiction between some experimental data and the dispersed barrier hardening theory<sup>(6)</sup> is discussed. The effect of both alloying and cold-work on irradiation hardening is reviewed in sections 4 and 5, respectively. The superposition of irradiation hardening and the hardening due to either alloying or cold-work is outlined. In section 6 the deformation behaviour of neutron irradiated copper and copper alloys is investigated. Studies connected with the deformation behaviour of both irradiated copper and copper alloys using tensile testing and transmission electron microscopy are summarized.

## 2. MECHANISM OF IRRADIATION HARDENING

The basic mechanisms of irradiation hardening in fcc metals, such as copper, nickel and gold, have been extensively studied<sup>(1)</sup>. The main conclusion of the studies concerning the critical resolved shear stress (CSS) is that the increase in the CSS, due to neutron irradiation, is caused by vacancy agglomerates which act as barriers to dislocation motion. Seeger<sup>(6)</sup> considered these small vacancy agglomerates as depleted zones ( $\sim 10 \text{ \AA}$ ) created by fast neutrons. During irradiation at temperatures where vacancies are mobile, these vacancy agglomerates grow into vacancy loops.

In the dispersed-barrier hardening model, proposed by Seeger<sup>(6)</sup>, the motion of dislocations under an applied shear stress ( $\tau$ ) is impeded by obstacles randomly distributed in the glide plane. The dislocations can overcome these obstacles either by the Orowan mechanism<sup>(7)</sup>, in which the dislocations bow out between the obstacles and then surround them, or by passing over them or cutting through them. In the passing or cutting mechanism, thermal activation can help in overcoming the energy barrier caused by the obstacles. This thermal activation decreases the force (F) necessary for the dislocations to pass over the obstacles.

The distribution of the dislocation obstacles can be correlated with the shear stress ( $\tau_s$ ) necessary to drive the dislocations through these obstacles as follows:

$$\tau_s = A_s \left( \frac{1}{l_s} \right) \quad (1)$$

where  $l_s$  is the average distance between obstacles in the slip plane.

For the Orowan mechanism,

$$A_s = \alpha \mu b \quad (2)$$

where  $\mu$  is the shear modulus,  $b$  is the Burgers' vector and  $\alpha$  is constant.

For the cutting or passing mechanism,

$$A_s = \frac{F(T, \epsilon)}{b} \quad (3)$$

In randomly distributed obstacles,  $\frac{1}{l_s}$  is proportional to the square root of the area density of the obstacles ( $N_s$ ), i.e.

$$\frac{1}{l_s} \propto (N_s)^{\frac{1}{2}} \quad (4)$$

Since the area density ( $N_s$ ) is proportional to the volume density ( $C_s$ ) of the obstacles, it can be concluded from equation (1) that, for dispersed barrier hardening,

$$\tau_s \propto (C_s)^{\frac{1}{2}} \quad (5)$$

The superposition of hardening due to irradiation with hardening of other origin such as alloying and cold-work will be discussed in the following sections.

### 3. DOSE DEPENDENCE OF CSS

The dispersed barrier hardening model proposed by Seeger<sup>(6)</sup> predicts a  $(\phi t)^{\frac{1}{2}}$  dependence of the CSS, where  $\phi$  is the neutron flux and  $t$  is the time of irradiation. In this model, the motion of dislocations under applied shear stress is hindered by randomly distributed radiation-produced barriers. The point defect clusters are considered to be barriers to dislocation motion; their concentration is assumed to be proportional to the fluence  $(\phi t)$ . It was shown that the CSS should be proportional to the square root of the dose at 0 K.

There is a discrepancy concerning the dependence of the CSS on irradiation dose  $(\phi t)$ . Diehl<sup>(2)</sup> showed that copper followed  $(\phi t)^{\frac{1}{2}}$  dependence, in agreement with Seeger's theory, while others<sup>(3,8)</sup> indicated that it follows a cube root dependence (i.e.  $(\phi t)^{1/3}$ ). A number of workers<sup>(9-12)</sup> have investigated the effect of neutron irradiation on the CSS. For small neutron doses, the irradiation-induced increase in the CSS of Cu was found to be proportional to the square root of the dose, as long as the obstacle concentration increased linearly with the dose<sup>(9-12)</sup>. However, a decrease in hardening rate was observed at high neutron doses. This was attributed to the saturation in the density of the depleted zones that are active as dislocation barriers.

Blewitt et al.<sup>(3)</sup>, Young<sup>(13)</sup> and Thompson and Paré<sup>(14)</sup> also investigated the dependence of the CSS on  $(\phi t)$  in the fluence range  $1.5 \times 10^{11} < \phi t < 1.3 \times 10^{20}$  n/cm<sup>2</sup> at a temperature of 303 K. The CSS was found to be proportional to  $(\phi t)^{1/3}$ , which is not in agreement with the square root dependence predicted by Seeger.

Makin and co-workers<sup>(15)</sup> attempted experimentally to correlate the CSS with the density of defect clusters produced in neutron irradiated copper as observed by transmission electron microscopy. Single-crystal tensile specimens and corresponding specimens for electron microscopy were irradiated together using the same dose ( $2.5 \times 10^{18}$  n/cm<sup>2</sup>) and examined after annealing for various times at 548, 579 and 609 K. A single linear relationship was found between the CSS at 4.2 K and the square root of the density of clusters less than 50 Å in diameter after annealing at the temperatures mentioned. For the larger clusters, which are thought to be interstitial loops, this linear relationship was not obtained. Better

results were obtained when the CSS was correlated with the cube of the large clusters. This indicates that the  $(\phi t)^{\frac{1}{2}}$  dependence of the CSS applies only when there are small defect clusters, and this is the condition for the dispersed barrier hardening theory proposed by Seeger<sup>(6)</sup>.

It can be concluded that the agreement of stress-dose dependence with the dispersed barrier model ( $\tau \propto (\phi t)^{\frac{1}{2}}$ ) is due to small defect clusters ( $< 50 \text{ \AA}$ ). The discrepancy in the data reported must be due to differences in experimental conditions, such as irradiation temperature, differences in reporting the neutron fluence, and material characteristics<sup>1</sup>.

#### 4. EFFECT OF ALLOYING ON IRRADIATION HARDENING

Studies on the basic mechanisms of irradiation hardening have been primarily focused on pure metals and generally using single crystals. Attempts are made to clarify the principal problems that arise in going from pure to alloyed metals to meet the requirements of various reactors. The superposition of solid solution hardening and irradiation hardening was investigated by irradiating copper-gold<sup>(18)</sup> and copper-aluminium alloys<sup>(4)</sup>.

##### Copper-gold Alloys:

Neutron irradiation hardening of copper-gold single crystals was investigated by Basu and Diehl<sup>(18)</sup>. The concentration of Au ranged between 0.3 and 10 at.%. Test pieces from Cu-Au alloys with concentrations of 0.3, 1, 3 and 10 at.% Au were irradiated at  $\sim 353 \text{ K}$ . The dependence of the CSS on neutron dose at two

1. In recent work<sup>(16,17)</sup> samples of zirconium alloys and stainless steels were irradiated together in one capsule at low temperature ( $\sim 323 \text{ K}$ ) up to a dose of  $1.43 \times 10^{20} \text{ n/cm}^2$ .  $(\phi t)^{\frac{1}{2}}$  dependence of the yield stress was obtained in stainless steels, while  $(\phi t)^{1/3}$  dependence was found in zirconium alloys. The agreement of stress-dose dependence in stainless steels, with the dispersed barrier model is probably due to the presence of small defect clusters in irradiated stainless steels, as was shown by transmission electron microscopy investigations.

deformation temperatures (90 and 295 K) was studied. The results are shown in Fig. (1) together with pure Cu. The CSS is plotted versus  $(\phi t)^{\frac{1}{2}}$ . A linear relationship appeared at small doses for the alloy crystals as well as for the pure copper single crystals. According to these plots, the authors stated that a linear superposition of alloy hardening and irradiation hardening exists according to the following equation:

$$\tau = \tau_1 + \tau_2 \quad (6)$$

where  $\tau$  is the total shear stress necessary to drive the dislocations in the as-irradiated alloy  
 $\tau_1$  is the shear stress necessary for moving the dislocations through the stress field resulting from alloying  
 $\tau_2$  is the shear stress necessary to push the dislocations over the obstacles resulting from irradiation.

In Fig. (1) the data actually show linear increase, in the CSS at small neutron doses, and the extrapolation of the linear parts of the curves to zero dose agrees well with the CSS of the unirradiated alloy crystals, but the additivity in the CSS for the superposition of solid solution hardening and irradiation hardening cannot be stated, since the straight portions are not parallel. The increase in the CSS due to neutron irradiation is affected by alloying gold with copper. The dose dependence of  $\tau$  at low doses decreased with increasing amounts of gold in copper. This can be due to either a decrease in the production rate of dislocation obstacles with increasing gold concentration, or a decrease of the effectiveness of the depleted zones as dislocation obstacles. The latter was preferred by Basu and Diehl<sup>(18)</sup>. They concluded that the depleted zones become smaller with increasing gold concentration. This is due to the shortening of the ranges of dynamic crowdions which play an important role in the formation of these zones<sup>(6)</sup>. Another feature of the results in Fig. (1) is that, at high doses, the tendency to saturation in irradiation hardening diminishes with increasing Au concentration.

The data in Fig. (1) (90 K) were replotted on double logarithmic paper to correlate the CSS with the neutron dose  $(\phi t)$ . This is shown in Fig. (2), from which the following relation was obtained:

$$\tau \propto (\phi t)^m \quad (7)$$

The exponent  $m$  decreased with increasing Au concentration. It decreased from 0.36 for pure Cu to 0.06 for 10% Au concentration.

Copper-aluminium Alloy:

Koppenaar<sup>(4)</sup> investigated the neutron irradiation hardening of copper-aluminium single crystals with aluminium concentrations 0.5, 5 and 14 at.%. Single crystals of these alloys were irradiated at  $\sim 333$  K to neutron doses of  $1.4 \times 10^{17}$ ,  $0.94 \times 10^{18}$ ,  $0.97 \times 10^{19}$  and  $0.98 \times 10^{20}$  n/cm<sup>2</sup>. The dose dependence of the CSS of these alloys is shown in Fig. (3), indicating the following:

1. The CSS of pure copper showed cube root dependence, i.e.  $\tau \propto (\phi t)^{1/3}$
2. The increase in  $\tau$  due to neutron irradiation decreases with the increase of Al concentration at low neutron doses  $\nu < 5 \times 10^{17}$  n/cm<sup>2</sup>
3. At high aluminium concentration (14 at.% Al), the CSS is neutron dose-independent when the dose is less than  $2 \times 10^{17}$  n/cm<sup>2</sup>, while the CSS is independent of solute concentration at high neutron doses ( $> 2 \times 10^{17}$  n/cm<sup>2</sup>).

In other publications, Koppenaar<sup>(19)</sup>, and Blewitt and Koppenaar<sup>(20)</sup> studied the superposition of alloy hardening and irradiation hardening in Cu-Al alloys. They re-interpreted the data of Koppenaar<sup>(4)</sup> according to the following superposition:

$$\tau^2 = \tau_1^2 + \tau_2^2 \quad (8)$$

where  $\tau_1$  is the stress necessary to drive the dislocation through alloying-produced obstacles  
 $\tau_2$  is the stress necessary to drive the dislocations through irradiation-produced obstacles.

In these publications, the CSS was plotted versus  $(\tau_{Al}^2 + \tau_1^2)^{-1/2}$ , where  $\tau_{Al}$  is the CSS of the unirradiated alloy and  $\tau_1$  is the CSS of irradiated pure copper. A reasonably good fit to a straight line was observed, supporting the validity of equation(8).



## 5. EFFECT OF COLD-WORK ON IRRADIATION HARDENING

The effect of pre-irradiation stressing on irradiation hardening of copper single crystals has been investigated by Blewitt et al.<sup>(3)</sup>, Essmann<sup>(21)</sup>, Koppenaal and Kuhlmann-Wilsdorf<sup>(5)</sup> and Brunner<sup>(22)</sup>.

According to Kuhlmann-Wilsdorf's theory<sup>(23)</sup>, the flow stress in work-hardened fcc metals is the stress required to multiply the dislocations by the Frank-Read mechanism. Work-hardening occurs due to the increase of the pinning points at which dislocations block the motion of each other. These pinning points increase with strain as the dislocation density increases. It is recognized that not all pinning points on dislocations are due to dislocation interactions, but additional types of pinning may exist. The additional pinning points of constant linear density on the dislocation line increase the flow stress, but do not increase the work-hardening rate.

Within the framework of this theory, irradiation hardening, after pre-irradiation stressing, can affect the CSS in different ways. The following possibilities have been suggested<sup>(5)</sup>:

1. Neutron irradiation causes strong pinning points on the existing dislocations at an average linear density of  $\frac{1}{l_i}$ . If the average linear density of pinning points between pre-existing dislocations is  $\frac{1}{l_p}$ , then the total linear density will be:  $\frac{1}{\lambda} = \frac{1}{l_i} + \frac{1}{l_p}$ , where  $l_i$  is the average distance between irradiation-produced pinning points and  $l_p$  is the average distance between pinning points produced by pre-existing dislocations. The stress at which the pre-existing dislocations are expected to bow out equals<sup>(23)</sup>:

$$\tau = \frac{Gb}{\pi\lambda} \quad (9)$$

where  $G$  is the shear modulus and  $b$  is the Burgers' vector. This equation can be put in the form:

$$\tau = \tau_i + \tau_p \quad (10)$$

$$\begin{aligned} \text{where } \tau_p \text{ (pre-irradiation stress)} &= \frac{Gb}{\pi l_p} \\ \tau_i &= \frac{Gb}{\pi l_i} \end{aligned}$$

2. The pinning of the pre-existing dislocations takes the form of an increased concentration of point defects. This increases the frictional stress for dislocation motion by  $\Delta\tau_F$ . The new stress will be:

$$\tau = \tau_p + \Delta\tau_F. \quad (11)$$

3. Irradiation generates point defects in the whole crystal, raising the frictional stress acting on the dislocation by  $\Delta\tau_F$ , and equation (11) applies.
4. In addition to the pre-existing pinning points  $N_p$  per unit area of slip plane, neutron irradiation produces strong pinning points of density  $N_i$ , randomly distributed over the slip planes. New dislocation multiplication requires the bowing of dislocations of an average length  $l$ , determined by the sum of the two pinning point densities, namely:  $l \propto (N_i + N_p)^{-\frac{1}{2}}$ . As  $l_i$  is proportional to  $N_i^{-\frac{1}{2}}$  and  $l_p$  is proportional to  $N_p^{-\frac{1}{2}}$ , the following equation can be obtained:

$$\tau^2 = \tau_i^2 + \tau_p^2. \quad (12)$$

5. Strong pinning points directly on the pre-existing dislocation give rise to equation (10), provided that the yield stress is determined by the bowing of the pre-existing dislocations. However, a different behaviour results if the irradiation damage depends on pre-existing dislocations, giving rise to permanent pinning points at the sites of these dislocations, but with the yield stress determined by the onset of further dislocations multiplication. In that case, the density of pinning points  $N_i$  must be proportional to the pre-existing dislocation density which in turn is proportional to  $l_p^{-2}$ . The average free length will be  $l \propto [N_p(1+\beta)]^{-\frac{1}{2}}$  with  $\beta$  a parameter incorporating the neutron dose and the cross-section for forming a pinning point at the dislocation core, so that:

$$\tau = \tau_p(1+\beta)^{\frac{1}{2}}. \quad (13)$$

Koppenaal and Kuhlmann-Wilsdorf<sup>(5)</sup> investigated the effect of pre-irradiation stressing on the strength of neutron-irradiated copper single crystals and discussed the above mentioned mechanisms. Copper single crystals with a purity of 99.999% were stressed before irradiation to  $\tau_p$  ranging from  $\sim 0.6 \text{ kg/mm}^2$  to  $\sim 5 \text{ kg/mm}^2$ . Some of these crystals, together with some annealed crystals of the same material, were irradiated at 333 K in the Argonne CP-5 reactor for about three days. After irradiation, the shear stress,  $\tau$ , of all specimens was determined. The results are illustrated in Fig. (4). The increase in CSS due to neutron irradiation was much higher for small values of  $\tau_p$  than for large ones. This indicates that the mechanisms described in items 1, 2 and 3 are not working, since  $\tau_i$  and  $\Delta\tau_F$  are constant for all specimens. The same also applies to the mechanism in item 5, since for higher  $\tau_p$ , the measured points approach a  $45^\circ$  line. This means that  $\beta$  in equation (12) equals zero. Also, the curve is not a straight line at the lower points. The results obtained are in good agreement with the mechanism in item 4. The best interpolation curve of the data in Fig. (4) is given by:

$$\tau = \Delta\tau_F + (\tau_i^2 + \tau_p^2)^{\frac{1}{2}}. \quad (14)$$

with  $\Delta\tau_F = 0.25 \text{ kg/mm}^2$  and  $\tau_i = 1.30 \text{ kg/mm}^2$ .

Koppenaal and Kuhlmann-Wilsdorf<sup>(5)</sup> concluded their work as follows:

1. The dominant obstacles produced by neutron irradiation, which act as pinning points, are produced in a random array in the lattice rather than principally on dislocations.
2. The CSS in neutron irradiated copper single crystals is governed by the stress required to generate dislocations rather than that required to move the pre-existing dislocations.

Brunner<sup>(22)</sup> investigated the effect of irradiation on the CSS of pre-irradiation-stressed pure copper (99.999%). Pure copper samples were deformed to flow stress  $\tau_p$  between 0.2 and 7.5  $\text{kg/mm}^2$ . The CSS of the samples was measured at 20 K after irradiation at low-temperature ( $\leq 20 \text{ K}$ ). Some of the results are shown in Fig. (5). For small pre-irradiation stresses ( $\tau_p < 1 \text{ kg/mm}^2$ ), additivity is observed between pre-irradiation stress and the increase of CSS due to irradiation (equation 11). In the range of small pre-

irradiation stress, the initial slope of the curves in Fig. (5) is unchanged, indicating that the deformation of the depleted zones is not influenced by the pre-irradiation deformation. S-shaped curves are observed at higher pre-irradiation stresses. At high neutron doses, these curves are parallel to the curves of annealed or slightly pre-irradiation-stressed samples.

Makin<sup>(23)</sup> reported measurements of the dose dependence of the yield stress of pre-irradiation-stressed polycrystalline copper samples. Qualitatively, the polycrystals show a behaviour similar to that of the single crystals in the work of Koppenaal and Kuhlmann-Wilsdorf<sup>(5)</sup>.

## 6. DEFORMATION OF NEUTRON-IRRADIATED COPPER AND COPPER ALLOYS

The deformation of neutron-irradiated copper crystals is characterized by coarse and widely-spaced primary slip lines and prominent cross-slip lines. Several studies concerning the deformation behaviour of copper single crystals have been carried out using stress-strain curves and replica techniques for studying surface slip lines<sup>(24,25,26)</sup>.

In general, the stress-strain curve of irradiated copper is characterized by an initial stage of constant stress where inhomogeneous slip takes place. This stage is called the "jerky flow" region or stage I. It is followed by a region of high work-hardening rate (stage II). This leads to a region of decreasing strain-hardening rate (stage III).

Transmission electron microscopy investigations on deformed irradiated copper crystals showed that the dislocations sweep out the irradiation-produced defects, leaving cleared channels.

The effect of a dispersed second phase on the deformation behaviour of irradiated copper crystals showed that the slip lines become irregular.

In the following, the deformation behaviour of neutron-irradiated copper and copper alloys is reviewed.

### Pure copper

A considerable number of investigations have been performed on the effect of neutron irradiation on the deformation of copper

single crystals. In unirradiated copper crystals, three work-hardening stages are observed. Stage I is characterized by small work-hardening rate, stage II by a rather high work-hardening rate, while in stage III, the work-hardening rate decreases continuously. These three stages are considerably changed by neutron irradiation.

Rukwied and Diehl made systematic studies<sup>(27-29,11)</sup> and showed that the work-hardening behaviour of neutron-irradiated copper single crystals is much more complicated than that of unirradiated crystals. Stage I was replaced by a yield point elongation zone. Stage II, which was characterized in the unirradiated crystals by a constant, high work-hardening coefficient, was subdivided after irradiation into a number of substages. Several linear portions with different work-hardening coefficients were observed.

Diehl and Hinzner<sup>(25)</sup> investigated this behaviour in detail. Cylindrical, copper single crystals (4 mm diameter) having similar orientation were irradiated to a neutron dose of  $5 \times 10^{17} \text{ n/cm}^2$  ( $E > 0.1 \text{ MeV}$ ). The crystals were tested in an Instron tensile-testing machine at room-temperature using a strain rate of  $1 \times 10^{-3} \text{ sec}^{-1}$ . The stress-strain curve of both irradiated and unirradiated crystals is shown in Fig. (6). The work-hardening stages and substages can be noticed. The yield point elongation zone is clear and followed by a portion with a considerably high work-hardening coefficient (substage IIa). The remaining part of stage II is divided into two linear substages. The first one (substage IIb) has a smaller work-hardening coefficient than the second (substage IIc), and these two substages have a lower work-hardening coefficient than substage IIa. At the beginning of stage III, a linear substage (IIIa) with a smaller work-hardening rate than in substage IIc is observed. After substage IIIa, the stress-strain curve approaches that of unirradiated crystals.

In a recent work, Howe<sup>(30)</sup> studied the deformation of copper single crystals irradiated to high doses. Cylindrical crystals of 2 mm in diameter were irradiated at 325 K to neutron doses of  $4 \times 10^{18}$ ,  $2.2 \times 10^{19}$ ,  $4 \times 10^{20}$  and  $8 \times 10^{20} \text{ n/cm}^2$  ( $E > 1 \text{ MeV}$ ). The as-irradiated crystals were pulled in an Instron machine at a strain rate of  $\sim 10^{-4} \text{ sec}^{-1}$ . In the stage I region, the flow stress was constant, the jerky flow was pronounced, and a Lüders' front advancing along the specimen produced coarse slip lines. This behaviour is similar to that observed in crystals irradiated to

lower neutron doses<sup>(3,27,31)</sup>. It was also noted that the CSS was relatively high and that the glide strain occurring in stage I before the start of linear hardening was large.

Using transmission electron microscopy techniques, Sharp<sup>(32)</sup> studied the deformation of neutron-irradiated copper single crystals. Cylindrical, single crystals of 3.5 mm in diameter were irradiated at 299 K to various doses. Most of the crystals were exposed to a neutron dose of  $1 \times 10^{18}$  n/cm<sup>2</sup> ( $E > 1$  MeV). Before irradiation, the crystals were annealed at 1123 K for one hour and slowly cooled to room-temperature. The as-irradiated crystals were polished and deformed to various strains using an Instron tensile testing machine at a strain rate of  $\sim 10^{-4}$  sec<sup>-1</sup> at 293, 77 and 473 K. Sections of 1 mm thickness, both parallel and normal to primary glide plane, were taken from the deformed crystals. Samples for electron microscopy (3 mm diameter) were obtained from these sections. Deformation occurred initially at all temperatures by the propagation of a Lüders' front where the slip lines on the surface are widely spaced. A new slip line forms well ahead of the existing lines and then rapidly develops into a small cluster of slip lines linked by cross slip.

All sections normal to the primary slip plane showed a high density of irradiation produced defects and defect-free channels parallel to the trace of a {111} plane. The widths of the channels were remarkably constant along their length. Different channels appeared to have slightly different widths. Within the cleared channels, dislocation debris was observed. Sections taken from crystals deformed to stage II also showed cleared channels and a high density of defects between the channels, as observed in stage I. Between the channels, however, many dislocations lying on secondary glide planes were observed. The distance between channels was less than that in stage I.

The slip band width determined by replica methods was smaller than the channel width as measured by transmission microscopy. However, slip band widths determined by replicas are subject to fairly large errors. The work of Makin and Manthorpe<sup>(31)</sup>, using an electron shadowgraph technique, indicates that the slip lines on the surface of the crystal deformed to the end of stage I after a dose of  $2.3 \times 10^{18}$  n/cm<sup>2</sup> have a width that is about the same as the observed channel width. The difference in data obtained by

replica and transmission electron microscopy may arise from the fact that the replica and thin foil are taken from different places in the specimen. It is interesting to note that the channel width decreased with decreasing deformation temperature and increasing neutron dose, while it is independent of strain rate at room-temperature.

In a recent work, Sharp<sup>(33)</sup> studied the correlation between cleared channels and surface slip steps in neutron-irradiated copper crystals. Cylindrical single crystals were neutron irradiated to a dose of  $2.5 \times 10^{18}$  n/cm<sup>2</sup> ( $E > 1$  MeV). A special electro-plating technique was used for preparing the specimens for the transmission electron microscope to show the relation between surface details and internal structure. After deformation to the end of stage I at room-temperature, the specimens were put in an electro-plating bath. Cleared channels were observed parallel to the trace of the primary slip plane. Each channel was found to terminate at a slip step on the surface. The channels were cleared of irradiation-produced defects for approximately the full width of the slip step indicating that the removal mechanism is relatively efficient.

In the work of Howe<sup>(30)</sup>, cleared channels were also observed lying parallel to the primary and cross-slip planes, after the deformation of highly irradiated ( $\phi t = 8 \times 10^{20}$  n/cm<sup>2</sup>) copper crystals. Even in the presence of a high defect density and a more complex damage configuration, it was possible for the glide dislocations to remove the defects in the same way as at lower fluences. Also, the measurements of channel width and spacing are in good agreement with the slip step measurements, thus indicating that there is indeed a one-to-one correspondence between the formation of a slip band and a cleared channel. This agrees with the results of Sharp<sup>(33)</sup>. It should also be noted that the slip band width, spacing and height increase with increasing testing temperature as does the average shear per slip band. A similar temperature dependence of slip parameters was noted by Sharp<sup>(33)</sup>.

### Copper Alloys

The deformation behaviour of neutron-irradiated copper alloys is different from that of neutron-irradiated pure copper. In general, the deformation of as-irradiated copper solid solution alloys has the following features:

1. The slip line pattern changes from homogeneous to heterogeneous with the formation and propagation of a Lüders' band.
2. The amount of "easy glide" stage increases.
3. The tensile axis overshoots indicating latent hardening on the secondary (conjugate) slip system.
4. The flow stress is more temperature dependent than in pure copper.
5. The formation of cleared channels decreases.
6. The slip line spacing decreases.
7. The average shear per slip line is smaller than in copper.

The effect of the addition of a dispersed second phase on the deformation behaviour of irradiated copper crystals has received little attention<sup>(4,34,35)</sup>. In general, the following features have been observed:

1. The formation and propagation of a Lüders' band.
2. A smoother stress-strain curve than in irradiated pure copper.
3. The formation of well defined groups of slip lines with large spacing before the end of stage I, where the surface of the crystal is filled with slip lines.
4. The slip lines are generally straight and interconnected by many cross slip segments.
5. The formation of cleared channels with smaller spacing than in pure copper.

In his work on the effect of neutron irradiation on the strength of  $\alpha$  Cu-Al single crystals, Koppenaal<sup>(4)</sup> investigated the deformation of copper-base alloys containing 0.5, 5 and 14 at % Al. The behaviour of the stress-strain curves of these alloys was similar to that shown in Fig. (7), indicating the following:

1. The formation of two Lüders' band similar to that observed in neutron-irradiated copper single crystals.
2. The amount of strain, with nearly constant stress, corresponding to the first Lüders' band extension, increased with neutron dose.
3. The rate of work-hardening during linear hardening decreased slightly with increasing neutron dose.
4. The stress corresponding to the initiation of the second Lüders's band increased with the neutron dose, but to a



lesser degree than the stress of the first Lüders' band formation.

Brimhall and Mastel<sup>(34)</sup> studied the deformation structure of neutron-irradiated copper-aluminium alloy (8% Al). The alloy was irradiated together with pure copper at 313 K to a neutron dose ranging from  $1 \times 10^{18}$  to  $1 \times 10^{19}$  n/cm<sup>2</sup>, and then pulled in an Instron tensile testing machine to a maximum strain of 5%. The deformed structure of the irradiated alloys was different from that of pure copper. In pure copper, the moving dislocations swept out the irradiation-produced defects forming free channels. Such defect-free channels did not appear in the irradiated alloy.

In a recent work, Sharp<sup>(35)</sup> studied the deformation behaviour of three different neutron-irradiated copper alloys, using mainly transmission electron microscopy. The alloys used were copper - 0.8% Cobalt single crystals containing equiaxed precipitates of diameter  $\sim 930$  Å, internally oxidized copper - 0.05% Al single crystals, and single phase Cu - 4% Al single crystals. All these crystals were irradiated at reactor ambient temperature to a neutron dose of  $1 \times 10^{18}$  n/cm<sup>2</sup>. The as-irradiated crystals were deformed in an Instron tensile testing machine at a strain rate of  $\sim 10^{-4}$  sec<sup>-1</sup> at room-temperature. Both the mean slip line spacing and the mean slip line height were measured using replica technique. Sections both parallel and normal to the primary slip plane were taken from the deformed crystals for electron microscopy. The following observations were made:

1. In all alloys, a Lüders' band propagated down the crystals at approximately constant stress.
2. Well defined groups of slip lines were formed with large spacing between groups, until at the end of stage I, the whole crystal was filled with slip lines.
3. The stress-strain curve was smoother in the alloys than in the irradiated copper crystals, especially in the internally oxidized copper-aluminium alloy (Cu-Al<sub>2</sub>O<sub>3</sub>).
4. Cross slip lines were frequently observed in all alloys except the Cu-4% Al (single phase).
5. The slip lines in the Cu-Co alloy were generally straight, interconnected by many cross slip segments. In Cu-Al<sub>2</sub>O<sub>3</sub> alloy, the straight segments were larger with shorter cross slip lines. In Cu-Al alloy, the slip lines were straight with a few isolated examples of short slip segments

parallel to cross slip planes.

6. Cleared channels appeared in all alloys except Cu-Al alloys. In the Cu-Co alloy, the width of the cleared channels is similar to that of irradiated pure copper, where the channels are straight and nearly uniform. In Cu-Al<sub>2</sub>O<sub>3</sub> alloy, the cleared channels are wider and irregular in width.

## 7. CONCLUSION

1. It is generally agreed that the increase in CSS due to fast neutron irradiation occurs according to the dispersed-barrier hardening model where the motion of dislocation under an applied shear stress is impeded by localized obstacles randomly distributed in the glide plane; this increase in CSS is proportional to the square root of the neutron dose.
2. The agreement of the stress-dependence on  $\phi t$  with the dispersed-barrier model exists when the irradiation-produced defects are small clusters  $< 50 \text{ \AA}$ .
3. The irradiation hardening rate is less in copper alloys than in pure copper; this hardening rate decreases with increasing solute addition.
4. The superposition of solid solution hardening and irradiation hardening is an alternative process for Cu-Al alloys where the higher CSS is the actual one; additivity was not ensured in Cu-Au alloys.
5. The superposition of hardening due to cold-work and irradiation hardening is, in some investigations, given by:

$$\tau^2 = \tau_i^2 + \tau_p^2,$$

where  $\tau_i$  is the CSS of irradiated copper, and  $\tau_p$  is the stress due to cold-work. However, in others, linear additivity exists between the pre-stress and the increase in yield stress due to irradiation.

6. Irradiation changes the stress-strain curve of copper,
-

where stage I is replaced by a yield point elongation zone with "jerky-flow", and stage II is replaced, after irradiation, by a number of substages with different work-hardening rates.

7. In irradiated copper crystals, the primary slip lines are coarse and widely spaced, cross-slip lines are prominent and the deformation is inhomogeneous as a Lüders' band propagates down the crystals.
8. During the deformation of irradiated copper crystals, the dislocations sweep out the irradiation-produced defects leaving cleared channels with a remarkably constant width.
9. The deformation behaviour of irradiated single-phase copper alloys is different from irradiated pure copper; the nature of slip line patterns changes from homogeneous to heterogeneous, the amount of "easy glide" increases, the formation of cleared channels and the slip line spacing decreases.
10. The addition of a dispersed second phase to copper causes a smoother stress-strain curve, the formation of cleared channels with irregular width and smaller spacing, and the formation of well defined groups of slip lines with large spacing before the end of stage I, where the surface of the crystal is filled with slip lines.

According to the reported data, the following points are suggested for further investigation:

- a. The dose dependence of the CSS and its relation to the size of irradiation-produced defects.
- b. The effect of pre-deformation on irradiation hardening in order to establish the mechanism governing the superposition of irradiation hardening and hardening due to cold-work.
- c. The deformation behaviour of irradiated copper and copper alloys during stage II.
- d. The effect of neutron irradiation on the strength and the deformation of second-phase copper alloys.

**ACKNOWLEDGEMENTS**

I wish to express my gratitude to H. Lilholt and B.N. Singh for their comments and helpful discussions. I am grateful to the Danish International Development Agency (DANIDA) for fellowhip support.

REFERENCES

1. J. Diehl, "Quench Hardening and Irradiation Hardening in FCC Metals", Vacancies and Interstitials in Metals, Proc. Int. Conf. KFA, Jülich (1968).
2. J. Diehl, Radiation Damage in Solids, Vol. I (IAEA, Vienna, 1969) 129.
3. T.H. Blewitt et al., J. Nucl. Mater., 2 (1960) 277.
4. T.J. Koppenaar, Acta Met., 12 (1964) 487.
5. T.J. Koppenaar and D. Kuhlmann-Wilsdorf, Appl. Phys. Lett. 4 (1964) 59.
6. A. Seeger, 2nd UN Int. Conf. of Peaceful Uses of Atomic Energy (Proc. Conf. Geneva, 1958) 6(1958) 250.
7. E. Orowan, Proc. Symp. of Internal Stresses in Metals and Alloys, the Institute of Metals, London (1948) 451.
8. D.O. Thompson and V.K. Paré, ORNL-384 (1963).
9. J. Diehl and W. Schilling, 3rd UN Int. Conf. of Peaceful Uses of Atomic Energy (Proc. Conf. Geneva, 1964) 9 (1965) 72.
10. J. Diehl, "The Influence of Neutron Irradiation on the Mechanical Properties of Face-Centered Cubic Metal Crystals", Radiation Damage in Solids I, IAEA, Vienna (1962) 129.
11. A. Rukwied and J. Diehl, Z. Metallk., 55 (1964) 266.
12. J. Diehl et al., Phys.Lett., 4 (1963) 236.
13. F.W. Young, J. Appl. Phys., 33 (1962) 3553.
14. D.O. Thompson and V.K. Paré, J. Appl. Phys., 36 (1965) 243.
15. M.J. Makin et al., Phil. Mag., 13 (1966) 729.
16. H.R. Higgy and F.H. Hammad, J. of Nucl. Mater., 44 (1972) 215.
17. H.R. Higgy and F.H. Hammad, J. of Nucl. Mater., 55 (1975) 177.

18. P. Basu, Thesis, Univ. Stuttgart (1969).
  19. T.J. Koppenaar, J. Appl. Phys., 35 (1964) 2750.
  20. T.H. Blewitt and T.J. Koppenaar, in Radiation Effects, (SHEELY, W.F.Ed.) Gordon and Breach, New York (1967) 561.
  21. U. Essmann, Phys. Stat. Sol., 3 (1963) 932.
  22. D. Brunner, Thesis (Diploma), Univ. Stuttgart (1968).
  23. M.J. Makin, in Radiation Effects (SHEELY, W.F.Ed.) Gordon and Breach, New York (1967) 627.
  24. I.G. Greenfield and H.G.F. Wilsdorf, J. Appl. Phys., 32 (1961) 827.
  25. J. Diehl and F. Hinzner, Phys. Stat. Sol., 7 (1964) 121.
  26. U. Essman and A. Seeger, Phys. Stat. Sol., 4 (1964) 177.
  27. J. Diehl, Radiation Damage in Solids, Vol. I, IAEA, Vienna (1962) 129.
  28. A. Rukwied, Z. Metallk. 55 (1964) 146.
  29. A. Rukwied, Z. Metallk. 55 (1964) 205.
  30. L. M. Howe, Radiation Effects, 23 (1974) 181.
  31. M.J. Makin and S.A. Manthorpe, Phil. Mag. 10 (1964) 579.
  32. J.V. Sharp, Phil. Mag., 16 (1967) 77.
  33. J.V. Sharp, Radiation Effects, 14 (1972) 71.
  34. J.L. Brimhall and B. Mastel, Appl. Phys. Letters, 9 (1966) 127.
  35. J.V. Sharp, Acta Met., 22(1974) 449.
-

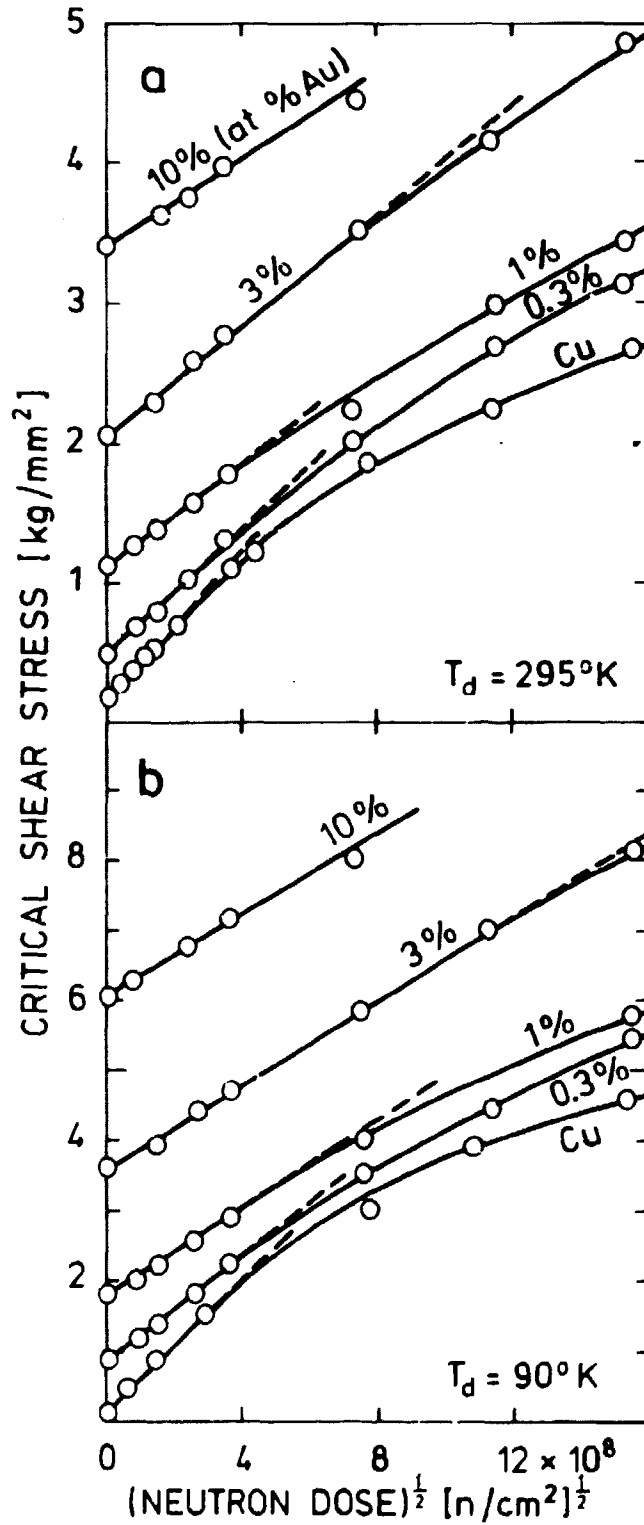


Fig. (1): Dependence of the CSS of copper-gold single crystals ( $\tau_0$ ) on the square root of the neutron dose ( $d^t$ ) for two deformation temperatures  $T_d$  and various Au concentrations.

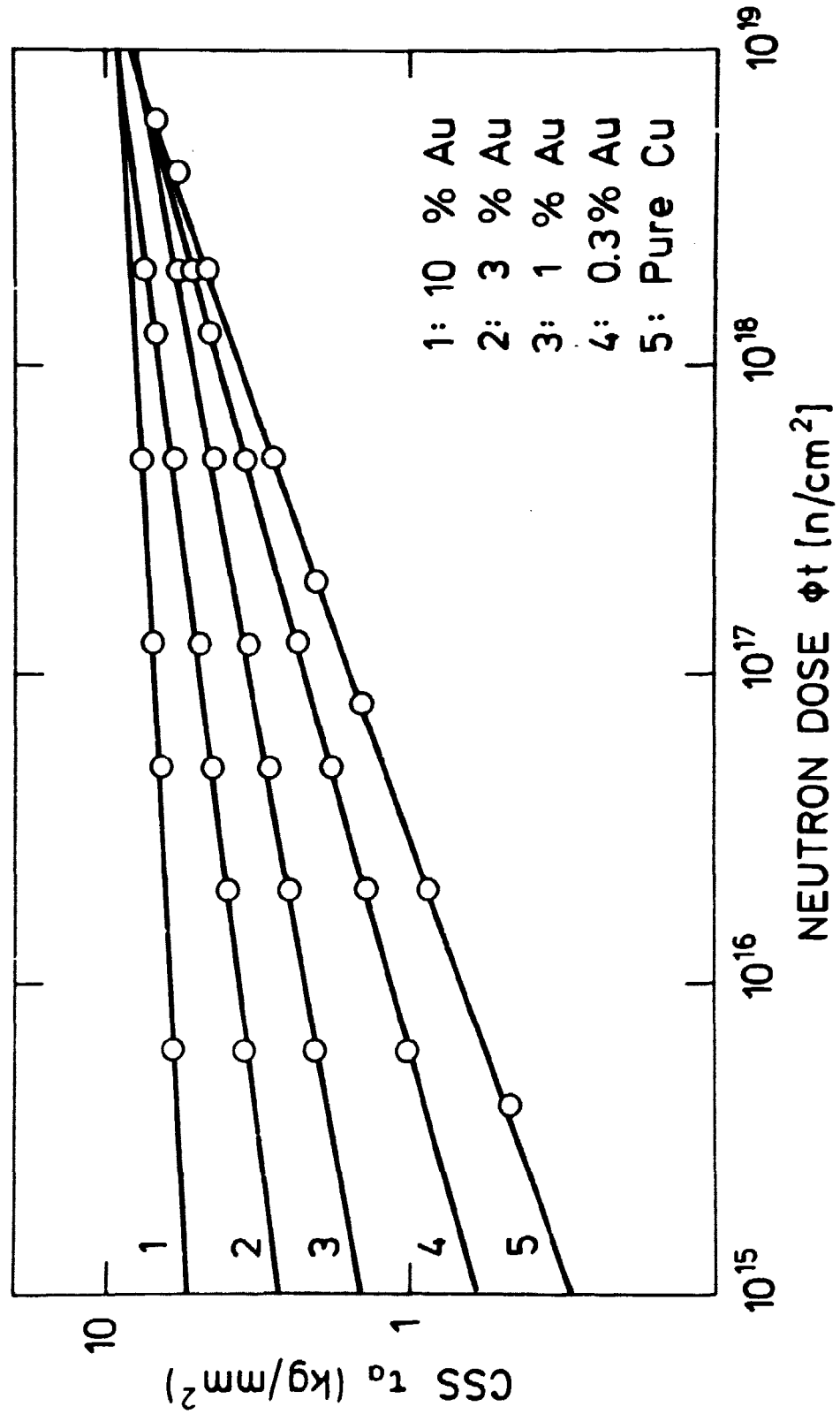


Fig. (2). Dose Dependence of the CSS of Cu-Au Alloys.



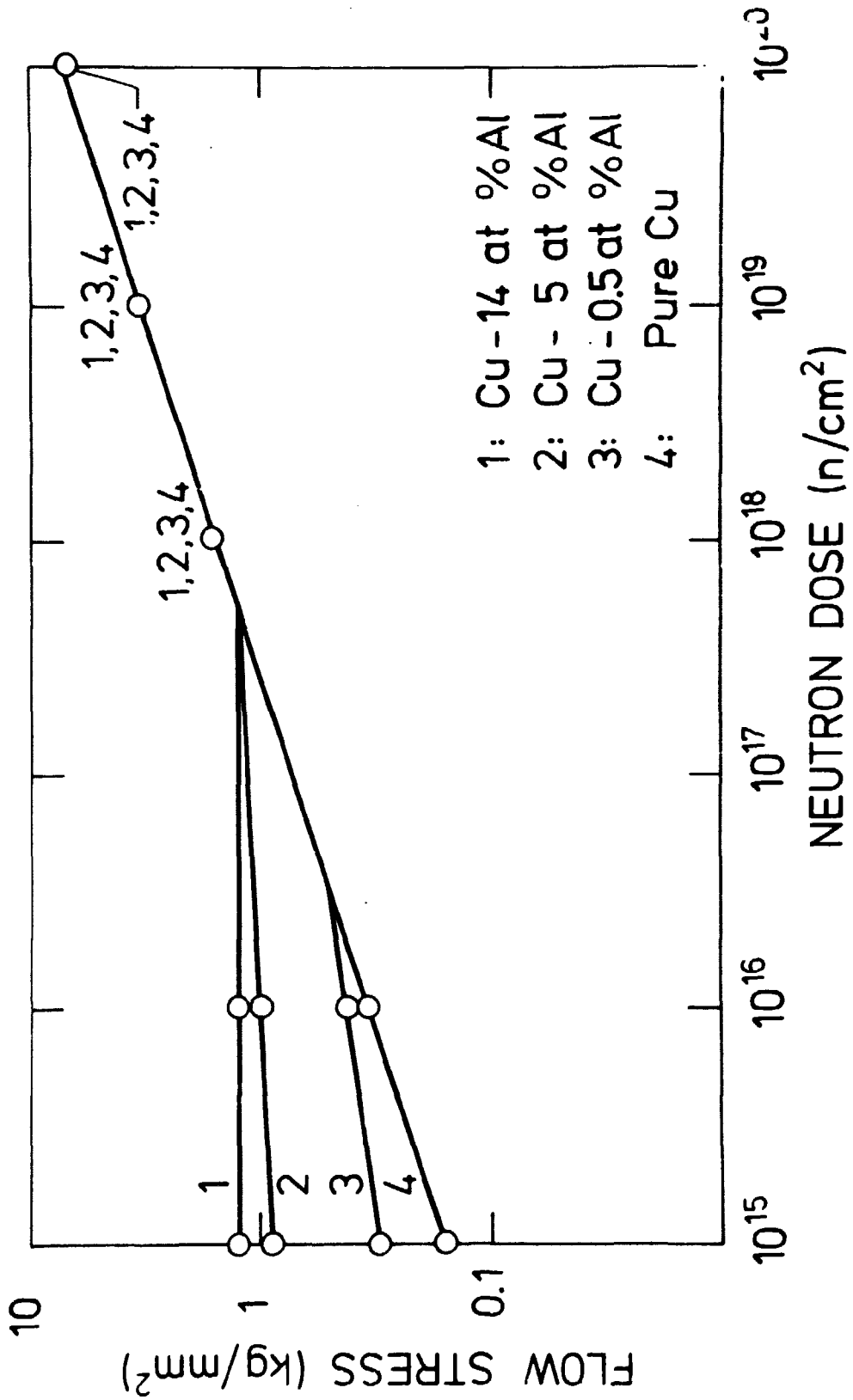


Fig. (3). Dose Dependence of the CSS of Cu-Al Alloys.

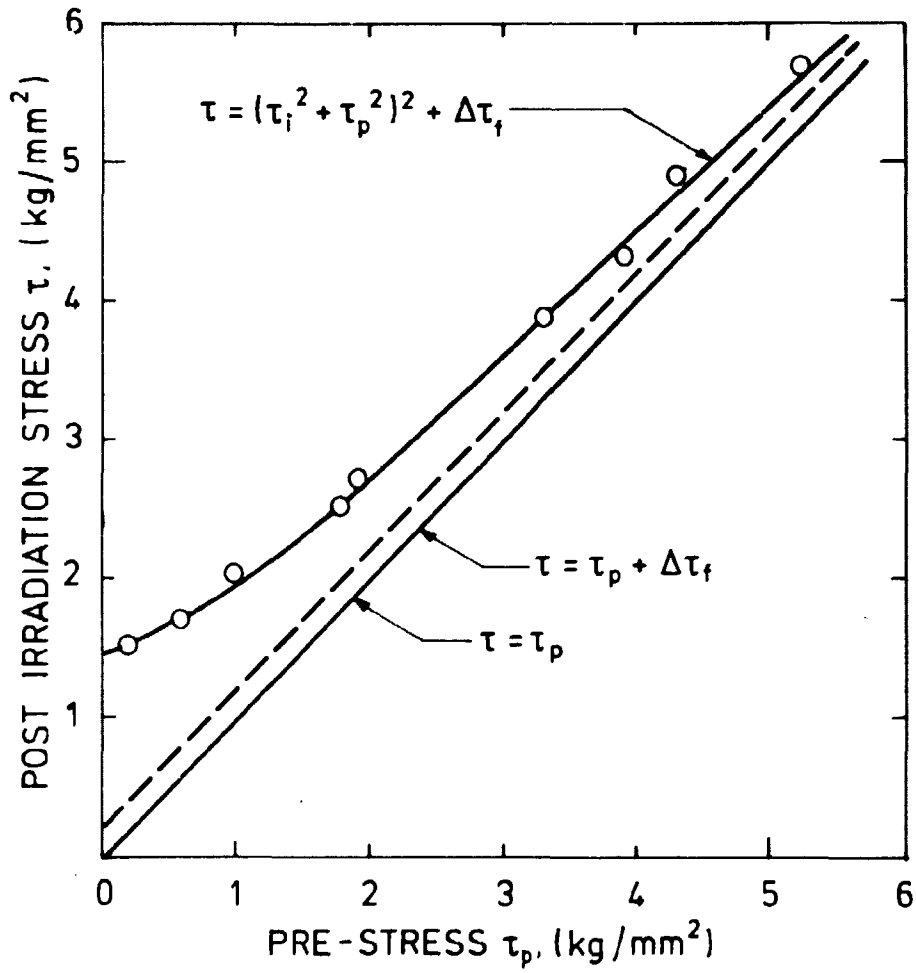


Fig. (4): The yield stress  $\tau$  in neutron-irradiated Cu single crystals vs pre-stress  $\tau_p$ .

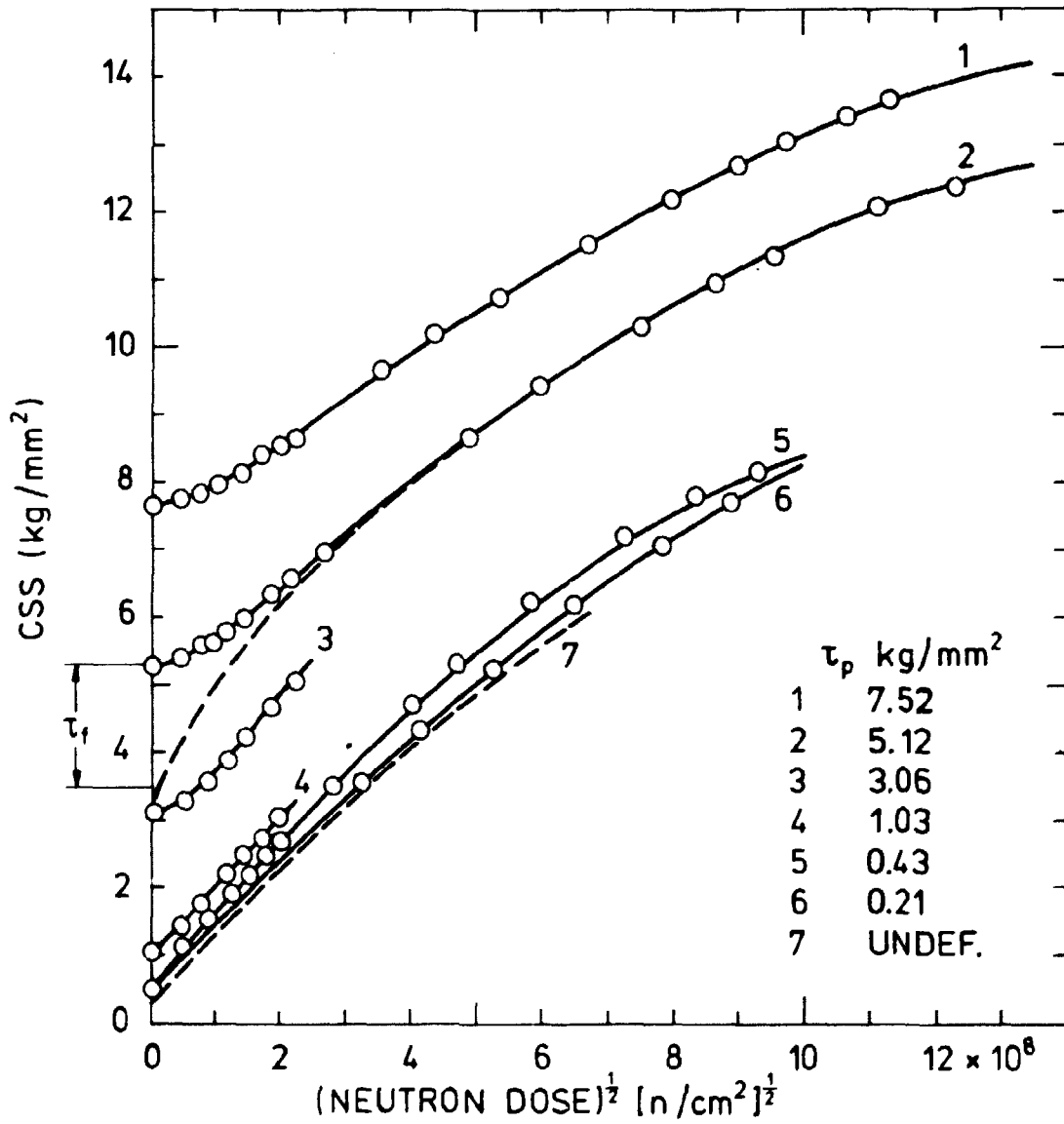


Fig. (5): Dose dependence of the CSS of copper single crystals, deformed prior to irradiation to various stress values  $\tau_p$ .

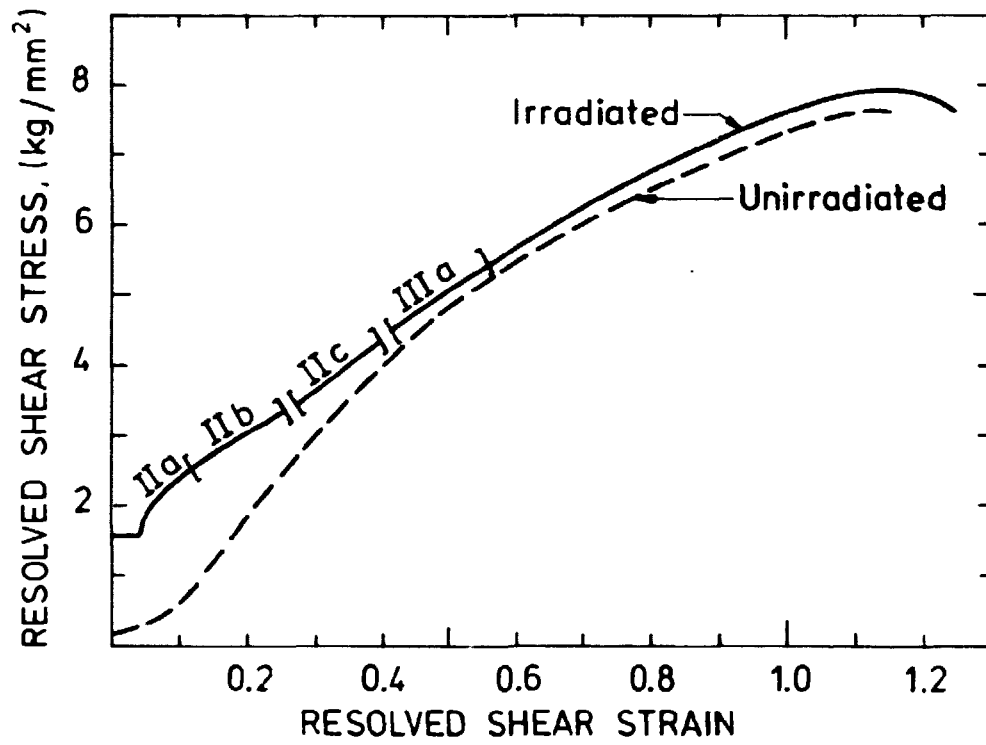


Fig. (6): Stress-strain curve of both irradiated and unirradiated copper single crystals.

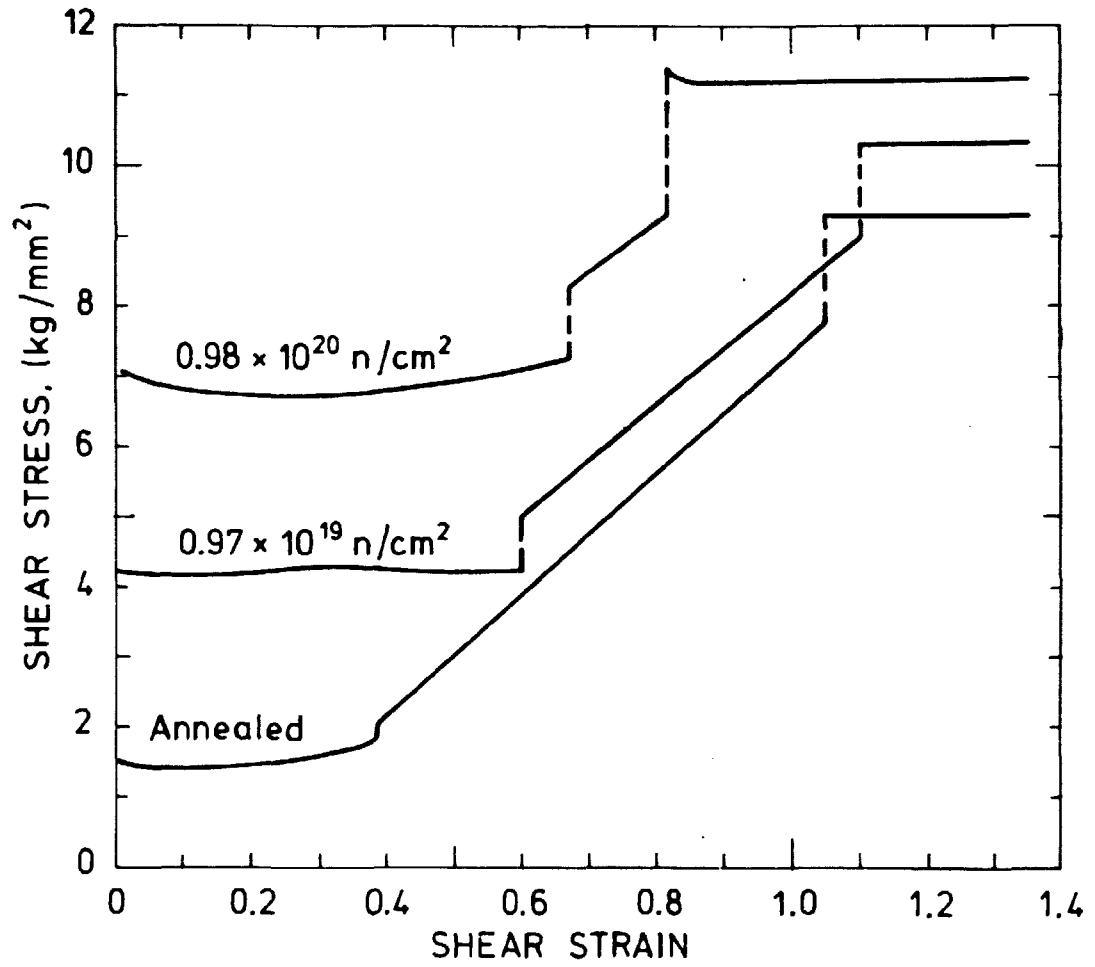


Fig. (7): Stress-strain curves for Cu - 14 at.% Al alloy.